

High-Speed Imaging in Biomedical Microfluidic Applications: Principles & Overview

By Kyle D. Gilroy, PhD · Field Applications Engineer · Vision Research Inc.

Microfluidics is a highly interdisciplinary field that employs state-of-the-art microfluidic chip technologies to guide fluid(s), and tiny objects within, through channels with micro-sized cross-sections. In the context of biomedical microfluidic applications, these tiny objects are most often cells with sizes within the range of one to one-hundred microns. Typical goals in this field involve tracking, identifying, sorting, diagnosing, and/or encapsulating individual cells. Success in mastering such feats demands an experimental setup that harmoniously integrates conventional microscopy techniques, carefully crafted microfluidic devices, and high-speed imaging technologies.

In our everyday world, nearly anybody can capture high-quality video of an object (for example a baseball) soaring through the air at 1 meter-per-second. On the microscale, however, imaging objects moving at that same speed is far more challenging. This is because capturing footage of speedy micro-objects often requires frame rates in the hundreds of thousands, and exposure times in the single-digit microsecond arena. As will become evident from the case studies discussed herein, collecting high-quality video data in biomedical microfluidic applications requires not only high- and ultra-high-speed cameras, but also the understanding of basic microfluidic-flow physics and imaging principles.

In the beginning of this paper, provided are a set of basic equations that can be used to approximate the fundamental physical principles involved in microfluidics. Then, summarized are a series of recent peer-reviewed publications where high-speed cameras were used to: track and quantify cell trajectory, observe cell stretching during deformability cytometry, guide and isolate circulating tumor cells, and encapsulate and sort individual cells.

FUNDAMENTAL IMAGING PRINCIPLES

Many of the challenges of imaging on the microscale are common to those faced in conventional high-speed photography. The primary differences are the greatly reduced field-of-view and much smaller object sizes. To obtain high-quality image data, it is paramount to (i) achieve sufficiently high frame rates, and (ii) reduce image blur caused by lengthy exposure times and/or quickly moving micro-objects. The origin of these challenges can be visualized in the schematic shown in **Figure 1**, which shows two sequential frames (*frame 1* and *frame 2*) of the same microsphere moving at a velocity of v_{sphr} through a microfluidic channel imaged at a frame rate of FR and with an exposure time of t_{exp} . Frame rate establishes the effective distance (d_{frame}) a microsphere travels between subsequent frame captures, as defined by:

$$d_{frame} = v_{sphr} \times (FR)^{-1} \quad (1)$$

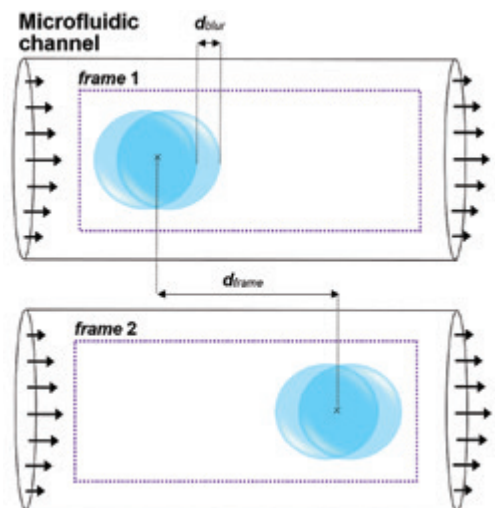


Figure 1: Schematic showing two sequential frames of a microsphere moving through a microchannel to illustrate the concept of motion blur and distance traveled between frames. In each frame, the trailing and leading sphere represent the instantaneous spherical profile at the start and end of exposure.

High-Speed Imaging in Biomedical Microfluidic Applications: Principles & Overview

If you were to mount a standard video camera atop a general-use laboratory microscope with a 10× objective lens, which typically has a round field-of-view with a diameter of 2 mm, you would find that imaging a micro-object (*i.e.*, a cell), moving linearly at the apparent ‘slow speed’ of 1 m·s⁻¹ (or equivalently 1 μm·μs⁻¹) would be extremely difficult. In fact, recording a video where at least 10 frames show a complete cell requires a minimum frame rate of *ca.* 5500 frames-

per-second (fps)! Furthermore, excessive exposure times (*e.g.*, ~100 μs) would make the cell appear as a streak instead of its natural round profile, which leads to a loss in valuable shape information. This is referred to as motion blur – an optical artifact that causes an object to appear elongated in the direction of motion. The blur-length (d_{blur}) of a microsphere, for example, is directly related to v_{sphr} , and the exposure time (t_{exp}), as defined by:

$$d_{blur} = v_{sphr} \times t_{exp} \quad (2)$$

Therefore, the percent motion blur (%*Blur*) of a 10 μm spherical cell moving at 1 μm·μs⁻¹ (with exposure time set to 10 μs) will be 100% in the direction of motion, as determined by the following equation:

$$\%Blur = 100 \times d_{blur} \times cell\ size^{-1} \quad (3)$$

In some emerging microfluidic applications, researchers are interested in capturing the motion of cells moving at up to 7 μm·μs⁻¹, which pushes the necessary frame rates into the hundreds of thousands, with micro- and submicro-second exposure times. These concepts are of critical importance in the sections below, especially when discussing the topic of *deformability cytometry*.

Overall, as a rule of thumb, before carrying out your microfluidics experiment, it is best to do some back-of-the-envelope calculations to estimate the *FR* and t_{exp} you will need based on approximate cell size and velocity, the field-of-view, and the minimum distance you want a cell to travel between sequential frames, with Eqs. 1 & 2.

EXPERIMENTAL SETUP

In many biomedical microfluidic applications, a syringe pump is used to provide a positive pressure on an inlet of a microfluidic chip, forcing cell-containing fluid from the syringe to percolate through the chip and eventually exit into a separate collection reservoir. A typical benchtop setup is shown in **Figure 2A**, which shows a syringe, and syringe pump, connected in series with a microfluidic chip that is back-lit by a high-intensity fiber-optic illuminator. Note: In this example, the sample is magnified through a Nikon SMZ18 microscope and imaged with a Phantom VEO 640S high-speed camera, but both bits of hardware are interchangeable. However, the most common way of interfacing a high-speed camera with a microscope is through a C-mount adaptor, which can be attached

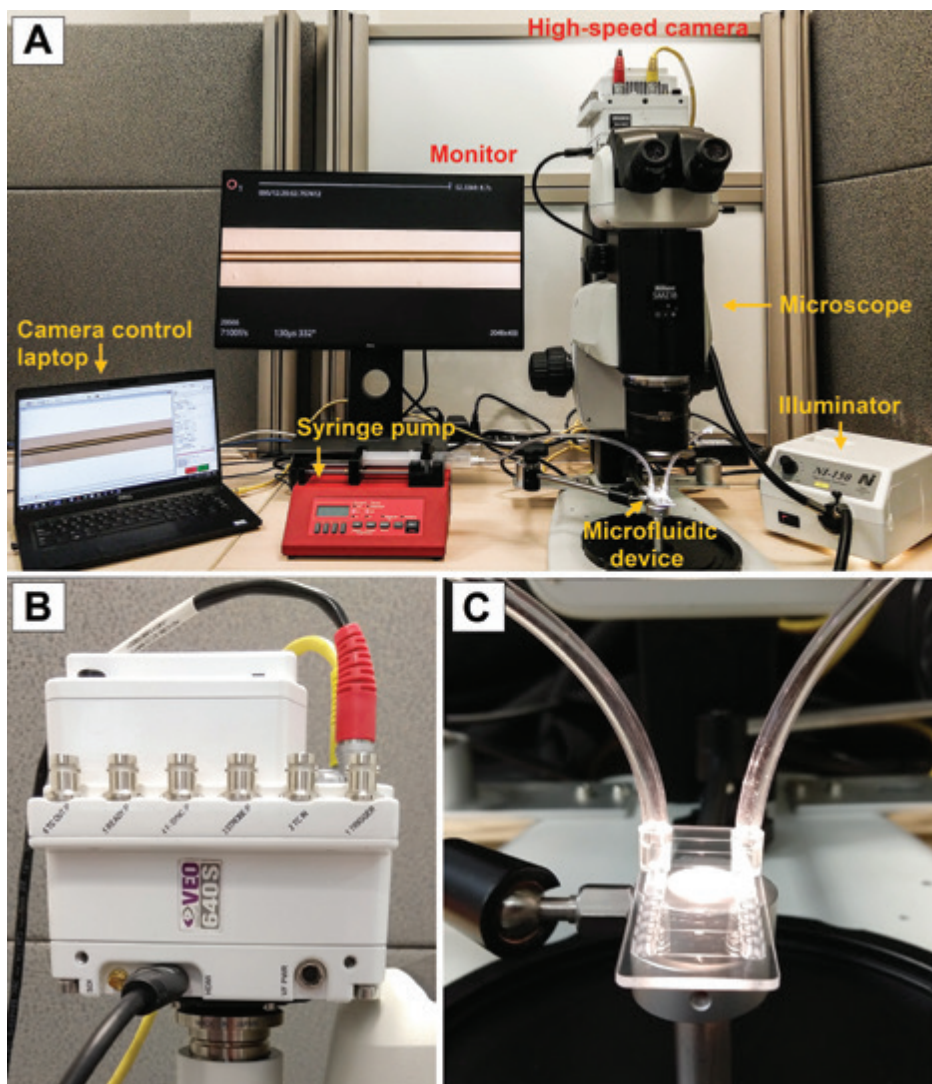


Figure 2: (A) Microfluidics setup, (B) close-up view of the high-speed camera, and (C) 8-channel microfluidic chip.

High-Speed Imaging in Biomedical Microfluidic Applications: Principles & Overview

to the face of the camera and then to a compatible microscope, see **Figure 2B**. This setup can be used with virtually any transparent microfluidic device, see **Figure 2C** for a close-up picture of a commercially available 8-channel chip.

One advantage over conventional high-speed imaging is the fact that intense backlighting can be used to avoid the common problem of light starvation seen in applications that rely on scattered photons arriving from light-sources placed at oblique angles with respect to the camera view. While this setup can be adapted for all sorts of biomedical microfluidic applications, each study will have their own unique equipment (e.g., pressure controller, camera, microscope, microfluidic device, etc.).

TRACKING CELL TRAJECTORY

One application in microfluidics is to observe and quantify the trajectory of cells within a microchannel network. Even as a seemingly straightforward application, quantifying the trajectory of cells moving through a microfluidic device can be quite complex. Interest in this field stems from the fact that knowing the position and velocity of cells traversing microfluidic channels can provide pertinent information regarding channel design, or even more interestingly, the biomechanical properties of cells (e.g., stiffness, adhesion, elasticity).¹ With this motivation, researchers from the Georgia Institute of Technology and Emory University demonstrated that the stiffness of cells flowing through a ridged-microfluidic channel could be directly correlated to the trajectory of the cell.¹ A schematic illustration of the microfluidic setup is shown in **Figure 3A**, which shows a syringe pump forcing a solution containing K562 lymphoblastic cells through a microfluidic device (at a concentration of 1 million cells·mL⁻¹ and flow rate of 50 μ L·min⁻¹). The resultant bright-field image was then magnified by a Nikon Eclipse Ti inverted microscope (20 \times) and directed to the sensing chip in

a Phantom v7.3 high-speed camera operating at 800 fps at a reduced resolution of 640 \times 480. Colored trajectories of three different cells are shown in **Figure 3B**.

In this case study, two experiments were performed with the only difference being the stiffness of the cells. In one experiment, normal K562 cells were flowed through the device, and another where softened K562 cells were used. To soften the cells, they were treated with the actin depolymerizing agent cytochalasin D. After analyzing and comparing the results, they concluded that the measured trajectories were strongly influenced by the stiffness of the cells, and furthermore, through computational modelling, the trajectory could be predicted. The derived algorithm was robust enough to handle the physics of cell collision and detachment events.

DEFORMABILITY CYTOMETRY

A lot can be learned from simply watching an individual cell undergo deformation. This is because certain cytoskeletal properties, which define the mechanical properties of a cell, are strongly influenced by cell state (e.g., healthy vs. diseased).^{2,3} Therefore, as argued by UCLA Professor Di Carlo and co-workers, deformability – degree of shape change under an applied stress, can be used as an effective biomarker for determining cell cycle stage, degree of cell differentiation, metastatic potential, and leukocyte activation.^{3,4} For example, cancer cells are typically more compliant than those that are benign, which endow them the ability to more easily move throughout the body *via* metastasis.^{5,6}

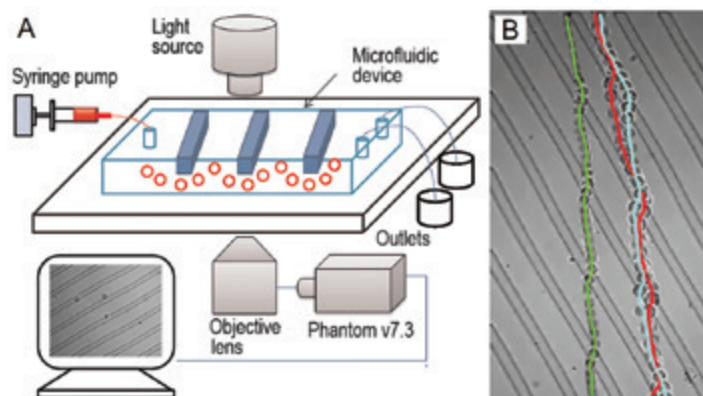


Figure 3: (A) Schematic illustration of the experimental setup. (B) Images showing a stack of frames to show trajectory of three individual cells. Images modified with permission from reference 1.

In another example, having the ability to measure deformability allows for establishing a distinction between healthy and malaria-infected blood cells, where those infected are known to be much stiffer than those not infected.^{5,7} Therefore, the correlation between deformability and *cell state* has researchers excited about the prospect of developing inexpensive label-free diagnostic techniques.

To illustrate this concept, researchers from the University of California fabricated a microfluidic device with an *extensional flow region* that could systematically deform fast-moving MCF7 cells (a breast cancer cell line), see **Figure 4, A and B** for the concept and a picture of the microfluidic chip, respectively.⁸ In this system, high flow rates could get the cell velocity to ca. 6.5 μ m· μ s⁻¹ (approximated from data shown in Figure 4C, the cell traveled ca. 91 μ m in 14 μ s). To capture such a fast-moving cell, a Nikon Eclipse Ti (10 \times objective) was interfaced with a Phantom v7.3 camera set to a frame rate of 142,857 fps, reduced resolution of 256 \times 32, and exposure time of 1 μ s.

As evident by the series of snapshots in **Figure 4C**, once the cell reached the extensional flow region (at $t = 28 \mu$ s), the cell underwent substantial stretching. This is quantified by measuring the longitudinal

High-Speed Imaging in Biomedical Microfluidic Applications: Principles & Overview

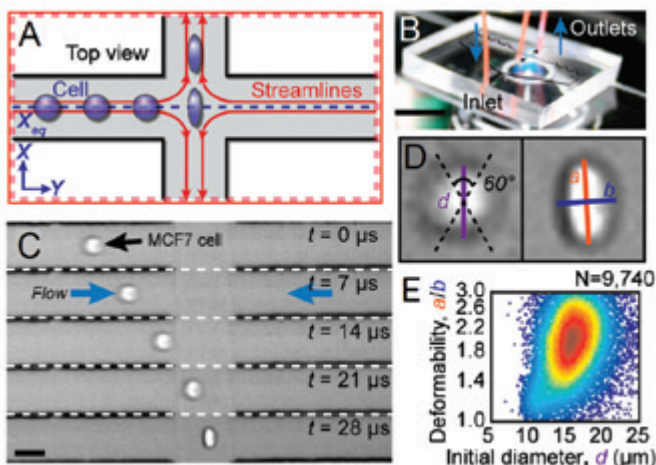


Figure 4: (A) Schematic of the extensional flow region, (B) photograph of the microfluidic chip, (C) snapshots of a cell entering the extensional flow region and then undergoing deformation, (D) close-up of deformed cell, and (E) density scatter plot. Note: the scale bars in B and C are 25 μm and 40 μm , respectively. Images reproduced with permission from reference 8.

and transverse axes (as defined in **Figure 4D**). By taking a closer look at the image data, the authors noted clear image blur along the direction of motion. The blurring of the cells was attributed to the 1 μs exposure time, because during each exposure, the cell moves roughly 6.5 μm (roughly 33% blur for a 20 μm cell, see **Eq. 3**). Despite the motion blur, measured values for deformability of *ca.* 2000 cells $\cdot\text{s}^{-1}$ could be measured, and computer processing was used to determine initial diameter and deformability of the cells, see a typical plot from such analysis in **Figure 4E**. In addition to the image blur, evident from **Figure 4C**, only five frames could be captured when the cell was in the field-of-view at the given reduced resolution. This is due to the high cell speeds of *ca.* 6.5 $\mu\text{m}\cdot\mu\text{s}^{-1}$, which at a frame rate of 142,857 fps, allows the cell to travel roughly 46 μm between frames (**Eq. 1**).

There is more than one way to deform a single cell using a microfluidic device. Outside from subjecting cells to an

extensional flow field as previously discussed, researchers from University at Albany and Rensselaer Polytechnic Institute recently took a different route by developing what they referred to as an *inertial microfluidic cell stretcher*.⁶ In this 2017 study, individual MDA-MB-231 breast cancer cells (among other cell types) were flowed at a rate of 450 $\mu\text{L}\cdot\text{min}^{-1}$ and made to collide with a rigid wall

at speeds of 4 $\mu\text{m}\cdot\mu\text{s}^{-1}$. Capturing video of the collision allowed the researchers to quantify the aspect ratio of the cell before and after the collision, and thus degree of deformation.

The rapid deformation process was captured using a Zeiss Axio Observer A1 inverted microscope (10x) interfaced with a Phantom v2512 configured to collect 3 s of footage at a frame rate of 100,000 fps with an exposure time of 1 μs . This enabled a throughput of *ca.* 450 cells $\cdot\text{s}^{-1}$. With the collected data, they utilized a custom algorithm to calculate initial cell diameter and deformability in a fully automated manner. The raw video data is freely available in the supporting information by visiting the website listed in reference 6.

ISOLATING CIRCULATING TUMOR CELLS

A promising way to detect and monitor certain types of cancers is by capturing circulating tumor cells (CTCs) in blood.⁹ CTCs enter the blood stream by shedding from a tumor site, after which

they migrate through the body and have the deleterious potential to nucleate new tumors.¹⁰ In fact, in a 2006 review article, metastasis was stated to account for 90% of deaths from those who have solid tumors.¹¹ Therefore, having the ability to detect, remove, and understand CTCs continues to be of great interest to many cancer researchers. Unfortunately, these cells typically represent only 1 to 100 cells in 10⁹ blood cells,¹² and are therefore very difficult to isolate and detect.

A collaboration between researchers from the Massachusetts Institute of Technology, and academic and health institutes of Singapore, worked on developing a microfluidic device with spiral-shaped channels capable of separating cells using centrifugal and lateral drag forces.^{12, 13} This process is referred to as: “Dean Flow Fractionation”, and is used to spatially segregate cells of different sizes within the cross-section of microchannels, see **Figure 5A** for the general concept.^{12, 14, 15} Then, by having a bifurcation at a proper down-stream location, for example cross-section A-A in **Figure 5A**, cells of specific sizes can be effectively directed down one of two pathways (*e.g.*, white blood cells (WBCs) vs. CTCs). In the example shown in **Figure 5**, the smaller cells could be directed toward the outer walls, whereas the larger

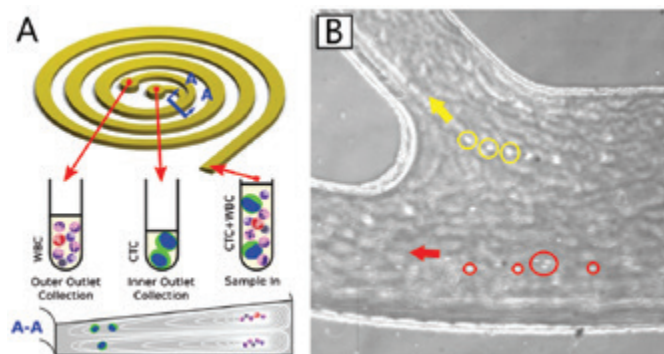


Figure 5: (A) Schematic of the concept, (B) snapshot of the microfluidic bifurcation showing MDA-MB-231 cells (some encircled in yellow) and white blood cells (some encircled in red) traveling in the top and bottom channel region of the bifurcation, respectively. Schematic and snapshot were taken from reference 13. Reproduced by permission of The Royal Society of Chemistry.

High-Speed Imaging in Biomedical Microfluidic Applications: Principles & Overview

CTCs could be concentrated at the inner wall. Using this technique, they showed that they could isolate greater than 80% of cancer cells in cell lines investigated, which included MCF-7, T-24, and MDA-MB-231 cells.¹³ The segregation process could be directly observed by interfacing an inverted phase contrast Olympus IX71 microscope with a Phantom v9 operating at 6400 fps.

In another publication, by connecting two cascaded spirals in series, 3 mL of whole blood could be processed within one hour with 100% CTC detection.¹² A clinical trial consisting of blood analyses of samples from twenty lung cancer patients also revealed successful detection, ranging from 5 to 88 CTCs·mL⁻¹.

ENCAPSULATING AND SORTING CELLS

Cells that are genetically identical can exhibit completely different behaviors.^{16, 17} Because of this fact, as stated by Chabert and Viovy, measurements performed on *bulk* cell populations provide incomplete insights.¹⁷ To better understand cell-to-cell variability, some research groups have focused on developing methods for isolating single-cells through encapsulation, which may eventually lead to methods for single-cell studies. For example, researchers at Institut Curie crafted a microfluidic device capable of encapsulating cells within picoliter-sized droplets, and then self-sorting them; a process driven completely by hydrodynamic effects.¹⁷

The researchers could capture the dynamic events by integrating an Olympus direct BX41 microscope (40x) with a Phantom 4.2 camera. As shown in **Figure 6A**, when a cell passes through the channel (indicated by the white arrows), it causes the jet neck to break, and a cell-filled droplet to form. At the same time, many smaller cell-empty droplets also form. However, after the two different types of droplets exit the channel, they are directed along two different pathways, see **Figure 6B**. Even

though the cell-filled droplets favor travelling down the top pathway (and cell-empty droplets favor the bottom), some of the relatively smaller cell-filled droplets can make it down the lower pathway, as pointed out by the white arrows in **Figure 6B**.

The authors showed that this technique has promise for real-life application by taking a whole blood mixture and then encapsulating and sorting cancerous T-lymphocytes. The authors also mentioned that the enrichment obtained using this device was insufficient for handling micrometastasis in the blood, but was high enough for genetic typing T cells infected with the human immunodeficiency virus (HIV).¹⁷

CONCLUDING REMARKS

Evident from these case studies, requisites for collecting quality video data from high-throughput biomedical microfluidic studies include having frame rates on the order of hundreds to hundreds-of-thousands of frames-per-second and exposure times in the single-digit microsecond arena. Even though our intuition may lead us to believe that a mere 1 meter-per-second micro-object should be easy to image, we can see from these studies that it is simply not the case.

In this article, spatial resolution was not discussed in detail because pixilation of the cells was clearly not a limiting issue. In general, cameras used in conventional microscopy can have resolutions up to 20 megapixels, which have pixel sizes of

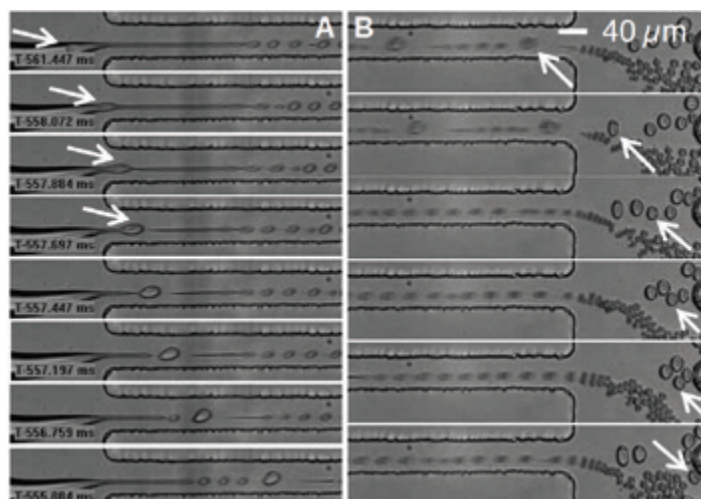


Figure 6: Snapshots showing the (A) jet neck breaking and encapsulation and (B) sorting process. Images were reprinted with permission from reference 17. Note: white arrows point to droplets including cells. Copyright (2008) National Academy of Sciences, U.S.A.

approximately 1 micron. These cameras provide excellent spatial resolution for static and slow-moving microscopy applications. However, for ultra-high-speed cameras, sensor resolutions are typically lower (e.g., 1 megapixel) with pixel sizes ranging between 20 and 30 microns. This permits significantly higher frame rates along with the sensitivity and image quality required to capture reliable image data. To increase the frame rates necessary for some high-speed biomedical microfluidics applications (e.g., > 100,000 fps), the resolution must be windowed down (for example: 640 × 480 or 256 × 32). Thus, there is still a need to achieve microscopy cameras with higher resolutions that at the same time achieve ultra-high frame rates.

One more consideration is the intrinsic limitation when imaging sub-micron-sized particles with visible light, as defined by the diffraction limit. When it comes to imaging objects with nanometer-sized dimensions, electron-based imaging is a must. However, frame rates achievable by conventional electron microscopes are still quite limited. Capturing high-resolution

High-Speed Imaging in Biomedical Microfluidic Applications: Principles & Overview

aberration corrected electron images, for example, typically takes up to ten seconds per frame, and the user typically remains completely motionless while hoping external laboratory vibrations are minimal to avoid noise. As technology continues to advance, it will be exciting to see instrumentation emerge capable of providing temporal and spatial resolutions for the next generation of cutting-edge applications where ultra-small and ultra-fast objects are involved.

I hope that this paper will bring beginner and intermediate researchers up to date with regards to recent research in this area, and serve as a basic guide for those who may have future interest in tackling their own high-speed microfluidics experiments.

NOTES

In each study discussed, the recorded video data is freely available in the form of supporting information, which can be accessed by following the links in the respective references. Copyright permissions were requested and granted from all publishers. This document is subject to change at any time.

ACKNOWLEDGEMENTS

This article was reviewed and edited by Toni Lucatorto, Gene Nepomuceno, and Phil Taylor.

References

1. J. Jeong, N. J. Froberg, E. Zhou, et al. *Accurately tracking single-cell movement trajectories in microfluidic cell sorting devices*, *PLoS ONE* **2018**, 13, e0192463. <https://doi.org/10.1371/journal.pone.0192463>
2. O. Otto, P. Rosendahl, A. Mietke, et al. *Real-time deformability cytometry: on-the-fly cell mechanical phenotyping*, *Nat. Methods* **2015**, 12, 199. doi:10.1038/nmeth.3281.
3. E. M. Darling, D. Di Carlo, *High-throughput assessment of cellular mechanical properties*, *Annu. Rev. Biomed. Eng.* **2014**, 17, 1. <https://doi.org/10.1146/annurev-bioeng-071114-040545>
4. D. Di Carlo, *A Mechanical Biomarker of Cell State in Medicine*, *J. Lab. Autom.* **2012**, 17, 32, DOI: 10.1177/2211068211431630.
5. S. Suresh, *Biomechanics and biophysics of cancer cells*, *Acta Mater.* **2007**, 55, 3989. <https://doi.org/10.1146/annurev-bioeng-071114-040545>
6. Y. Deng, S. P. Davis, F. Yang, et al. *Inertial microfluidic cell stretcher (iMCS): Fully Automated, high-throughput, and near real-time cell mechanotyping*, *Small* **2017**, 13, 1700705. <https://doi.org/10.1002/sml.201700705>
7. H. A. Cranston, C. W. Boylan, G. L. Carroll, et al. *Plasmodium falciparum maturation abolishes physiologic red cell deformability*, *Science* **1984**, 223, 400. DOI: 10.1126/science.6362007.
8. D. R. Gossett, H. T. K. Tse, S. A. Lee, et al. *Hydrodynamic stretching of single cells for large population mechanical phenotyping*, *Proc. Natl. Acad. Sci. USA* **2012**, 109, 7630. <https://doi.org/10.1073/pnas.1200107109>
9. S. L. Stott, C.-H. Hsu, D. I. Tsukrov, et al. *Isolation of circulating tumor cells using a microvortex-generating herringbone-chip*, *Proc. Natl. Acad. Sci. USA* **2010**, 107, 18392. <https://doi.org/10.1073/pnas.1012539107>
10. C. L. Chaffer, R. A. Weinberg, *A perspective on cancer cell metastasis*, *Science* **2011**, 331, 1559. DOI: 10.1126/science.1203543.
11. G. P. Gupta, J. Massagué, *Cancer Metastasis: Building a Framework Cell*, **2006**, 127, 679, DOI:10.1016/j.cell.2006.11.001.
12. H. W. Hou, M. E. Warkiani, B. L. Khoo, et al. *Isolation and retrieval of circulating tumor cells using centrifugal forces*, *Sci. Rep.* **2013**, 3, 1259. doi:10.1038/srep01259.
13. M. E. Warkiani, G. Guan, K. B. Luan, et al. *Slanted spiral microfluidics for the ultra-fast, label-free isolation of circulating tumor cells*, *Lab Chip* **2014**, 14, 128. DOI: 10.1039/C3LC50617G.
14. S. S. Kuntaogodanahalli, A. S. S. Bhagat, G. Kumar, et al. *Inertial microfluidics for continuous particle separation in spiral microchannels*, *Lab Chip* **2009**, 9, 2973. DOI: 10.1039/B908271A.
15. A. Russom, A. K. Gupta, S. Nagrath, et al. *Differential inertial focusing of particles in curved low-aspect-ratio microchannels*, *New J. Phys.* **2009**, 11, 9. doi:10.1088/1367-2630/11/7/075025.
16. J. M. Raser E. K. O'Shea, *Noise in gene expression: Origins, consequences, and control*, *Science* **2005**, 309, 2010. DOI: 10.1126/science.1105891.
17. M. Chabert, J.-L. Viovy, *Microfluidic high-throughput encapsulation and hydrodynamic self-sorting of single cells*, *Proc. Natl. Acad. Sci. USA* **2008**, 105, 3191. <https://doi.org/10.1073/pnas.0708321105>

VISION
RESEARCH

AMETEK®
MATERIALS ANALYSIS DIVISION



ABOUT VISION RESEARCH

Vision Research designs and manufactures digital high-speed cameras that are used in a variety of professional industries and applications. Vision Research is a business unit of the Materials Analysis Division of AMETEK Inc.

Certain Phantom cameras from AMETEK Vision Research are held to export licensing standards. For more information please go to: www.phantomhighspeed.com/export